

Investigation of core-loss mechanisms in large-scale ferrite cores for high-frequency applications

Michael Baumann, Christoph Drexler, Jonas Pfeiffer, Jens Schuelitzke, Erwin Lorenz and Michael Schmidhuber

SUMIDA COMPONENTS & MODULES GMBH

Dr. Hans-Vogt-Platz 1
94130 Obernzell, Germany
Tel.: +49 8591 937 – 441
Fax: +49 8591 937 – 9403
E-Mail: cdrexler@eu.sumida.com
URL: <https://www.sumida.com>

Acknowledgements

The authors would like to thank the Federal Ministry for Economic Affairs and Climate Action. Parts of the work presented here were done within the project with the funding code 03EI4014C.

Keywords

«Ferrite», «Finite-element analysis», «Magnetic device», «Core loss», «Core loss modelling», «Automotive component», «Dielectric loss»

Abstract

In this paper, core-loss mechanisms in ferrite cores are investigated. It is demonstrated that ferrite materials showing almost identical core-losses in the datasheets exhibit a completely different loss-behavior when cores with large cross-sections are manufactured. Therefore, there is a high risk that the wrong ferrite material is selected in the design process of a magnetic component for power electronic applications when only the losses from the datasheets are considered. Consequently, a model is developed which leads to a better understanding of the origin losses in ferrite cores and can be used as powerful tool to design and optimize magnetic components for high-frequency applications.

With this model, formulas are derived which allow the calculation of two additional loss contributions which are the electrical polarization losses and the volume eddy current losses. In a detailed experimental study of various ferrite core shapes and sizes the model is verified and clearly shows that for example at 100kHz with a magnetic cross-section of 500mm², the additional losses cannot be neglected. The dependencies and input parameters are discussed in detail. Finally, a FEM-based workflow is presented and verified by calorimetric measurements. In the future, this workflow can be used to precisely predict the losses of virtual prototypes in a development process i.e., for automotive applications.

Introduction

With the availability of SiC- and GaN-switches, a lot of effort has been spent to increase the switching frequencies of power electronic systems. While on the one hand the converted power can be increased in such novel systems, on the other hand it was often said to be obvious that the size of the magnetic components can be decreased in the same manner. However, it was discovered and reported recently [1] that the core losses drastically increase in the range of several hundreds of kHz making ferrite cores thermally unstable and the design process of such magnetic components much more difficult.

The development process of inductive components has been improved over decades and is summarized e.g., in [2-4]. A lot of effort has been made to develop methods to calculate the losses of ferrite cores in such components. The most popular approach is known as the Steinmetz-formalism, where sets of measurements are evaluated by phenomenological equations. Methods to estimate additional contributions due to eddy-currents have been addressed recently as well [5,6]. By contrast, models with a physical origin like the Play-model [7], which is an improved version of the Preisach-model, or the Jiles-Atherton-Model [8], among many others not mentioned here, have been developed over decades. However, all these models are typically benchmarked with ring-cores and often show weaknesses when it comes to a comparison with a large-scale ferrite-core. Thus, in a conventional design process of a magnetic component, the lack of accuracy of the models lead to iterative loops of assembly and testing of hardware prototypes which cost time and money.

In this paper, the mechanisms of core-losses in ferrite cores are presented and quantified. Based on 3D-finite-element-method (FEM) simulations, the core-loss density of PQ50-cores and other frequently used core shapes manufactured of SUMIDA high-frequency power ferrites is determined and experimentally verified. The findings give a better understanding about the loss-mechanisms in ferrite cores and close the gap between measurement and calculation. The presented method might serve as a powerful tool to investigate virtual prototypes in a modern development process for magnetic components.

Motivation

The focus of this paper is on the quantitative comparison of core-losses derived from finite-element-method simulations and calorimetric measurements. With the tendency addressed above to shrink the size of magnetic components for power electronic systems, the understanding of the loss-mechanisms in the core i.e., in ferrite-cores, are becoming more and more important. It is a known secret that there are huge discrepancies between losses in small size toroidal cores used for datasheet value measurements and large-scale cores used for applications. This manifests itself in the comparison of two ferrite materials presented in Fig. 1.

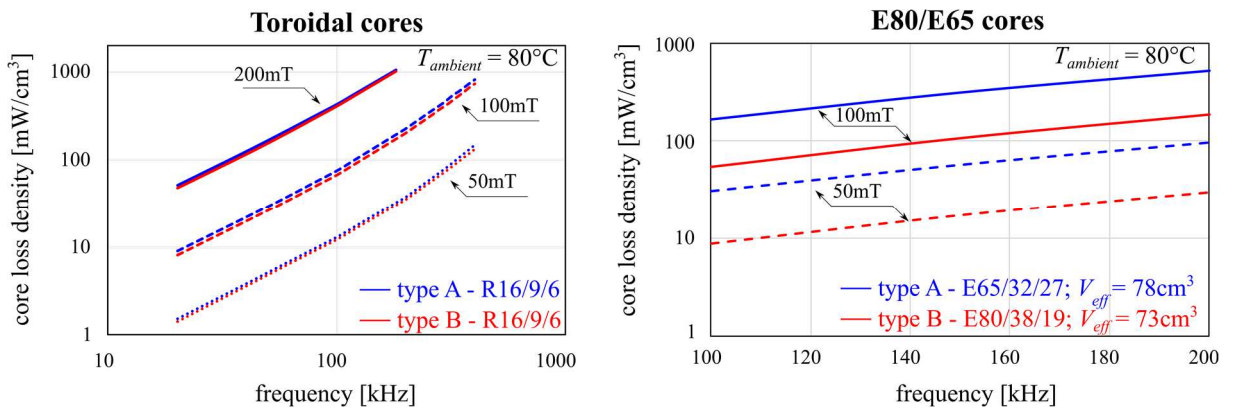


Fig. 1: Power loss density measurement of toroidal cores (left) and E-cores (right) for two SUMIDA ferrites at different peak flux densities: type A - high saturation flux density ferrite (blue) and type B - low loss high frequency ferrite (red). Both sets of measurements have been measured following standard DIN EN62044-3 for core temperatures of 80 °C.

Therein, the comparison of core-loss density measurements for two different SUMIDA power ferrite materials ($\mu_{\text{eff}} \approx 2000$) are presented. The first one is a ferrite with a high saturation flux density and is in the following called type A. The second one is a material which is optimized towards low losses at frequencies up to 400 kHz and is called type B. From those measurements it follows, that for small toroidal cores (left-hand side) the losses are almost the same with less than 5 % deviation for the considered temperature and frequency range. Hence, the materials look almost identical regarding the expected core losses. However, measurements of an E80-core of type B and an E65-core of type A (right-hand side) yield a difference in the core loss density of a factor of 3 to 4. It has to be mentioned

that the E-cores have not a perfectly identical shape but have almost the same effective volume. Consequently, similar core-losses would be expected by using the Steinmetz formalism. Therefore, there is a significant risk that the less-effective material could be selected in a development process when relying just on data derived from small-scale toroidal measurements. The findings give rise to having a closer look on the microscopic mechanisms behind the core losses and to deriving methods to predict the losses of magnetic components upfront in virtual prototypes.

Core-loss mechanism in ferrite cores

A common approach for the losses of ferrite cores is the separation in hysteresis, eddy-current and residual losses [4]:

$$P_{core} = P_{hyst} + P_{eddy} + P_{res} \quad (1)$$

Therein, the hysteresis losses are ascribed to losses due to the change of the magnetic moments with time. The eddy-currents are losses due to the non-zero conductivity of the ferrite and residual losses arise due to a phase shift between the external magnetic field and the oscillating magnetic moments at high frequencies being often neglected. In [1], a correction factor to the Steinmetz-approach was derived which accounts to the eddy-current losses and closes the gap between simulated and measured core-losses. However, this approach is non-physical and can be seen rather as a rule-of-thumb.

In this work, an additional core-loss contribution is investigated which will be in the following entitled as dielectric volume losses. Therefore, Eq. (1) can be re-written:

$$P_{core} = P_{hyst} + P_{(eddy,grain)} + P_{res} + P_{dielectric} \quad (2)$$

Herein, $P_{(eddy,grain)}$ accounts to the eddy current losses on grain-level which depend on the material compound. These losses do not depend on the geometry of the core and are already considered in the approach of the Modified Steinmetz Equation (MSE) for datasheet values. The additional term $P_{dielectric}$ is related to dielectric volume losses and will be derived and explained in the following chapter.

Deriving of dielectric volume loss

In [2] a derivation of eddy current losses for a rectangular cross-section based on the field equations is shown. However, the part of losses due to electric polarization is not considered. In the following, a simple method is shown, which also includes the electrical polarization loss component. The following derivation is only valid for Power-MnZn-Ferrite such as type A and type B where the penetration depth is still fully given due to the high resistivity and limited magnetic cross-section [9].

For a sinusoidal magnetic flux density B , an angular frequency ω and with the magnetic cross-section A_e (Fig. 2) a voltage U_{eff} is induced:

$$U_{eff} = \frac{\omega \hat{B} A_e(x)}{\sqrt{2}} = \frac{\omega \hat{B} \cdot 2x(l-d+2x)}{\sqrt{2}} \quad (3)$$

The resistant R of concentric loops of the geometric shape shown in Fig. 2 can be described with the specific resistant ρ as:

$$R = \frac{2\rho l}{dA_R(x)} = 2\rho \frac{(l-d)+8x}{bdx} \quad (4)$$

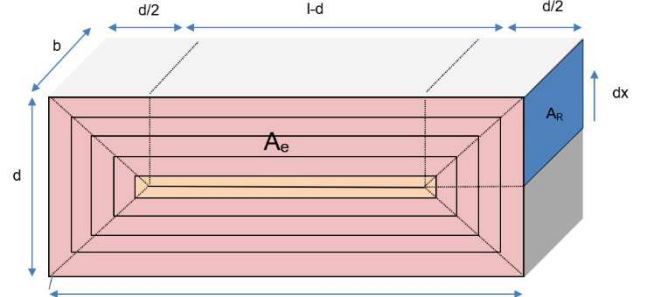


Fig. 2: Magnetic cross-section with integration loops

The movement of electrons due to the conductivity results in power losses:

$$dP = \frac{U_{eff}^2}{R} = \frac{4\pi^2 f^2 \hat{B}^2 b(l-d+2x)^2 x^2}{\rho(l-d+4x)} dx \quad (5)$$

Dividing by volume $V_e = lbd$ and integrating over dx , the specific power losses P_v can be calculated:

$$P_v = \frac{\pi^2 f^2 \hat{B}^2}{16\rho} \cdot \frac{64}{ld} \int_0^{d/2} \frac{2lx^2 - 2dx^2 + 4x^3}{l-d+4x} dx = \frac{\pi^2 f^2 \hat{B}^2}{16\rho} \left[\frac{(l-d)^4}{4ld} \ln \frac{l+d}{l-d} - \frac{(2l-2d)^2}{4} \right] \quad (6)$$

By introducing the effective magnetic cross section $A_e = ld$ and a geometric factor of the shape F_G

$$F_G = \frac{(l-d)^4}{4(ld)^2} \ln \frac{l+d}{l-d} - \frac{l^2 - 4dl + d^2}{2ld} \quad (7)$$

Eq. (6) can be written:

$$P_v = \frac{\pi^2 f^2 \hat{B}^2 A_e F_G}{16\rho} \quad (8)$$

A good simplification for F_G gives following equation with the help of the aspect ratio $F = l/d$:

$$F_G \approx \frac{8}{3F} - \frac{5}{3F^{1.7}} \quad (9)$$

In first approximation F_G can be further simplified with:

$$F_G \approx \frac{3}{F+2} \quad (10)$$

If, in addition to the electrical conductivity losses, dielectric polarization losses also occur, both loss mechanisms can be combined into an effective dielectric loss ϵ''_r [10]:

$$\epsilon''_r = \epsilon''_{dipol} + \frac{\sigma}{\epsilon_0 \omega} \quad (11)$$

The effective dielectric loss can be regarded as a high-frequency conductivity σ_{hf} [10]. The frequency-dependent part of conductivity can be neglected in case of MnZn-ferrite and used frequencies.

$$\sigma_{hf} = \epsilon_0 \omega \epsilon''_{dipol} + \sigma \quad (12)$$

Since the electric field not only acts on the ionic conductivity, but also on the dipolar conductivity, high-frequency conductivity can be used in the loss formula (8):

$$P_{dielectric} = \frac{\pi^2 f^2 \hat{B}^2 A_e F_G (\epsilon_0 \omega \epsilon''_{dipol} + \sigma)}{16} = \frac{\epsilon_0 \pi^3}{8} \left(\epsilon''_{dipol} + \frac{\sigma}{2\pi f \epsilon_0} \right) f^3 \hat{B}^2 A_e F_G \quad (13)$$

The simplest form with $\epsilon'' = \epsilon_0 \epsilon''_r$ and the help of (10) is:

$$P_{dielectric} = \frac{3\pi^3 \epsilon''}{8} f^3 \hat{B}^2 \frac{A_e}{F+2} \quad (14)$$

If the magnetic cross-section or the flux density along the magnetic path is not constant, then the individual volume elements must be described in sections where the most general form is:

$$P_{dielectric} = \frac{\pi^3 \epsilon'' f^3}{8V_e} \sum_{i=1}^n \frac{\hat{\phi}_i^2 l_i}{F_{G_i}} \quad (15)$$

In (12), one contribution is related to the material's conductivity σ and is in the following referred to as $P_{eddy,volume}$ and describes eddy currents which spread in the whole core-volume due to the conductive connection of single grain boundaries. Another contribution depends on the imaginary part of the

dielectric function ε''_{dipol} of the core material and will be called P_{dipol} in the following. Both parameters are dependent from temperature and frequency. A_e is the effective cross section of the core and F describes the length-ratio of the core's cross section and will be called aspect-factor in the following. F is equal to one for circular and square-shaped cross-sections and increases for rectangular shapes with the increasing difference of the side-lengths.

Experimental investigation of the dielectric volume loss

In order to investigate the additional losses experimentally, several tens of toroidal cores and U-cores of material type A and B were produced. The effective cross section of these samples ranges from 25 to 890 mm² and the geometric form-factor F is between 1 (circular or quadratic) and 4 (rectangular). The core-losses for all these designs were measured for different frequencies, flux-densities and temperatures following standard DIN EN62044-3 (see Fig. 3). Several hundreds of measurement points were acquired with that method. In parallel, the core-losses were calculated, in a first step, without the additional losses and are plotted against the measured losses in Fig. 4 (red points).

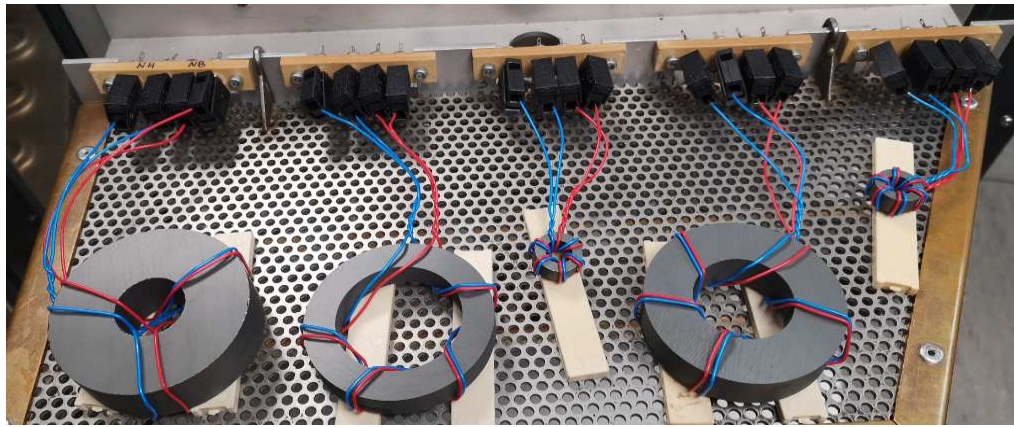


Fig. 3: Toroidal cores with different effective cross section in the experimental setup of the core-loss measurement

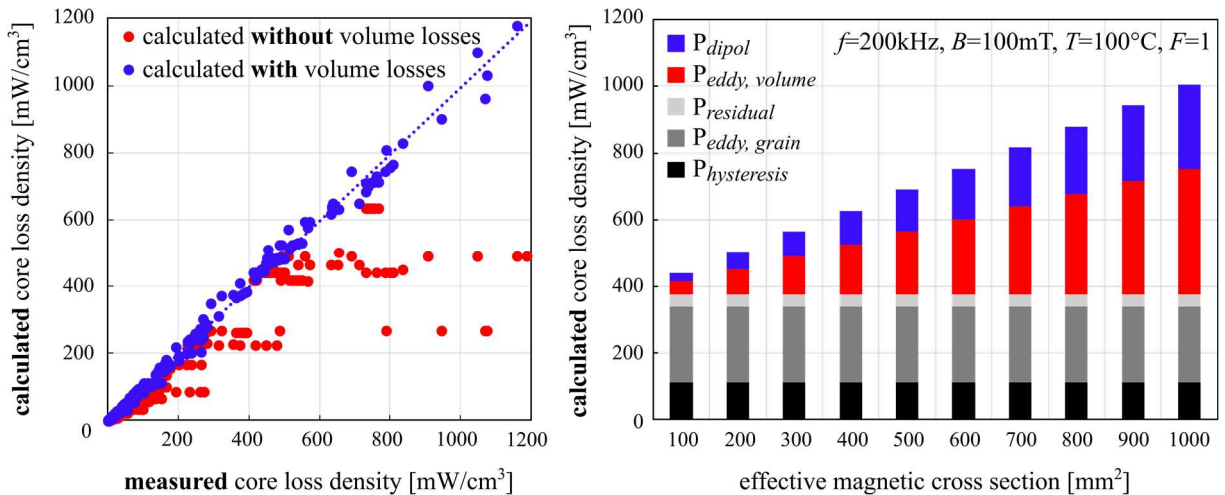


Fig. 4: left: Comparison of calculated and measured core-losses with (blue) and without (red) dielectric losses; each point represents either a toroidal core or a U-core with different cross-sections and produced of different ferrite materials; each core was measured/calculated at different points of operation under variation of frequency, flux-density and temperature; the dashed line reflects sufficient match of calculation and measurement; right: magnitudes of each contribution for ferrite-type B at a single point of operation and different cross-sections.

In this presentation method each point appearing on a line with a slope equal to one (dashed blue line) has a perfect agreement between measurement and calculation. It follows that a huge number of designs can be found far of that line when the dielectric volume losses are not considered (red points). It is not shown in the framework of this paper that especially at high-frequencies all designs with large cross-sections and/or low geometric form-factors show deviations up to a factor of three.

It is obvious from Eq. (14) and (15) that for the calculation of the additional losses the numbers for the effective dielectric loss ε''_r needs to be known. Hence, measurements need to be performed in order to extract these values which are presented in the next chapter.

Determination of the parameters for the dielectric volume loss

The effective dielectric loss ε''_r is a material parameter depending on temperature, frequency and conductivity and can be determined for several ferrite materials via measurements of small ferrite samples according to DIN 53483-2 reported by [11]. In the diagram Fig. 5 (left) an example for a Low-loss-MnZn-Ferrite is given. For simplification the Eq. (11) can be used to separate ε''_r in a part of conductivity loss $\sigma/(\omega\varepsilon_0)$ and in a part of polarization loss ε''_{dipol} shown in Fig. 5 (right). In this case the advantage is that ε''_{dipol} is in a first approximation independent of frequency f , temperature T and magnetic flux density B in the range between 50 kHz and 400 kHz and between 80 °C and 125 °C.

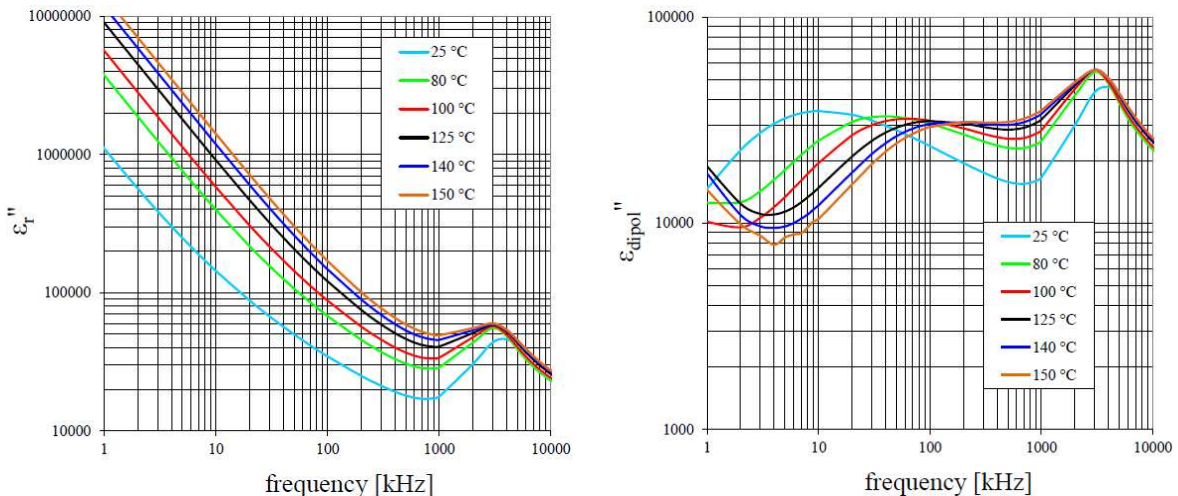


Fig. 5: Example of effective dielectric losses and electric polarization; left: Effective dielectric loss ε''_r in dependence on frequency and temperature according to DIN 53483-2; right: Electric polarization loss ε''_{dipol} in dependence of frequency and temperature according to Eq. (11)

The temperature dependence of the conductivity $\sigma(T)$ respectively the specific resistance $\rho(T)$ can be expressed by using the well-known Arrhenius-equation:

$$\rho(T) = \rho_\infty e^{E/k_B T} \quad (16)$$

with the Boltzmann constant k_B and the activation energy $E = 0,2 \text{ eV}$ which is in first approximation constant for Power-MnZn-ferrites [12]. The limit resistance ρ_∞ is given by using (16) with the usually available resistant $\rho(25^\circ\text{C})$. In Table I a comparison between the determination of ρ_{25} and ε''_{dipol} via small signal measurement and high-power measurement is done.

Table I: Dielectric polarization loss ϵ_{dipol}'' in dependence of frequency and temperature according to Eq. 10

Small signal DIN53483-2		High power Regression (Fig. 5Error! Reference source not found.)	
$\rho_{25^\circ\text{C}}$	$\epsilon_{\text{dipol}}''$	$\rho_{25^\circ\text{C}}$	$\epsilon_{\text{dipol}}''$
Type A ferrite	4 Ωm	60.000	5 Ωm
Type B ferrite	13 Ωm	30.000	10 Ωm

FEM-analysis and calorimetric measurements of core-losses

In the final chapter of this paper, the quantitative comparison of core-losses derived from finite-element-method simulations and calorimetric measurements is presented. Therefore, PQ50-cores of SUMIDA made of Fi395 medium-frequency power-ferrite are investigated. The DUTs are assembled with an airgap in order to improve the signal quality of the frequency generator. A litz-wire with 630 strands with a diameter of 0.1 mm is used for the winding to keep the winding losses low. In the experiment, a rectangular voltage is applied to the DUT and the corresponding peak flux-density is calculated from

$$B_{max} = \frac{U}{4A_{eff}N_f} \quad (17)$$

The temperature of the core is measured with type-K sensors at the center and the outer leg, respectively. More details about the calorimetric measurements can be found in [1].

In the simulations, a current source is used which directly injects a triangular current to the winding model which coincides with the amplitudes from the experiments to enable a one-by-one comparison of simulation and measurement. Both the spatial and the temporal distribution of the magnetic flux density is determined in a transient magnetoquasistatic analysis using the 3D-FEM-simulation tool JMAG. The hysteresis losses are evaluated with the formalism of the Modified Steinmetz Equation (MSE) following [2]. The volume eddy current and the electric polarization called dielectric losses are calculated element by element with the formulas derived above. The temperature rise is determined in an iterative thermal and magnetic simulation loop with a modified loss density distribution. For the thermal simulations, a simplified thermal equivalent circuit is used which assumes heat dissipation by free convection only (Fig. 6). The heat transfer coefficients are calculated following [12] or by empirically determined values. The simulation workflow is presented in Fig. 6. For more precision of the thermal simulation, a conjugate heat transfer solver can be used to accurately describe the convection of the sample. However, this step is too time-consuming for the presented workflow and therefore, out of scope of this paper.

Two plots with the results of simulated and measured losses of a PQ50-core are shown in Fig. 7. The first set of data demonstrates the increase of the losses with the magnetizing current and resulting flux density at a constant frequency of 200 kHz. It should be noted that for higher flux densities than 110 mT the core becomes thermally unstable due to the excessive self-heating. In another plot of Fig. 7 the frequency of the magnetizing current was changed but the amplitude was adjusted to keep the losses and thus, the temperature almost constant. The simulation results clearly show that the hysteresis losses calculated by the MSE (red points) underestimate the measured losses by almost 40 %. It must be noted that the component's winding is made of litz-wire in order to keep the winding losses (yellow circles) low which are calculated as described in [1]. From the authors point of view, the huge discrepancy

cannot be explained with the often-mentioned process deviations of ferrite cores or any statistical variations of the component's electrical parameters or any calculation errors.

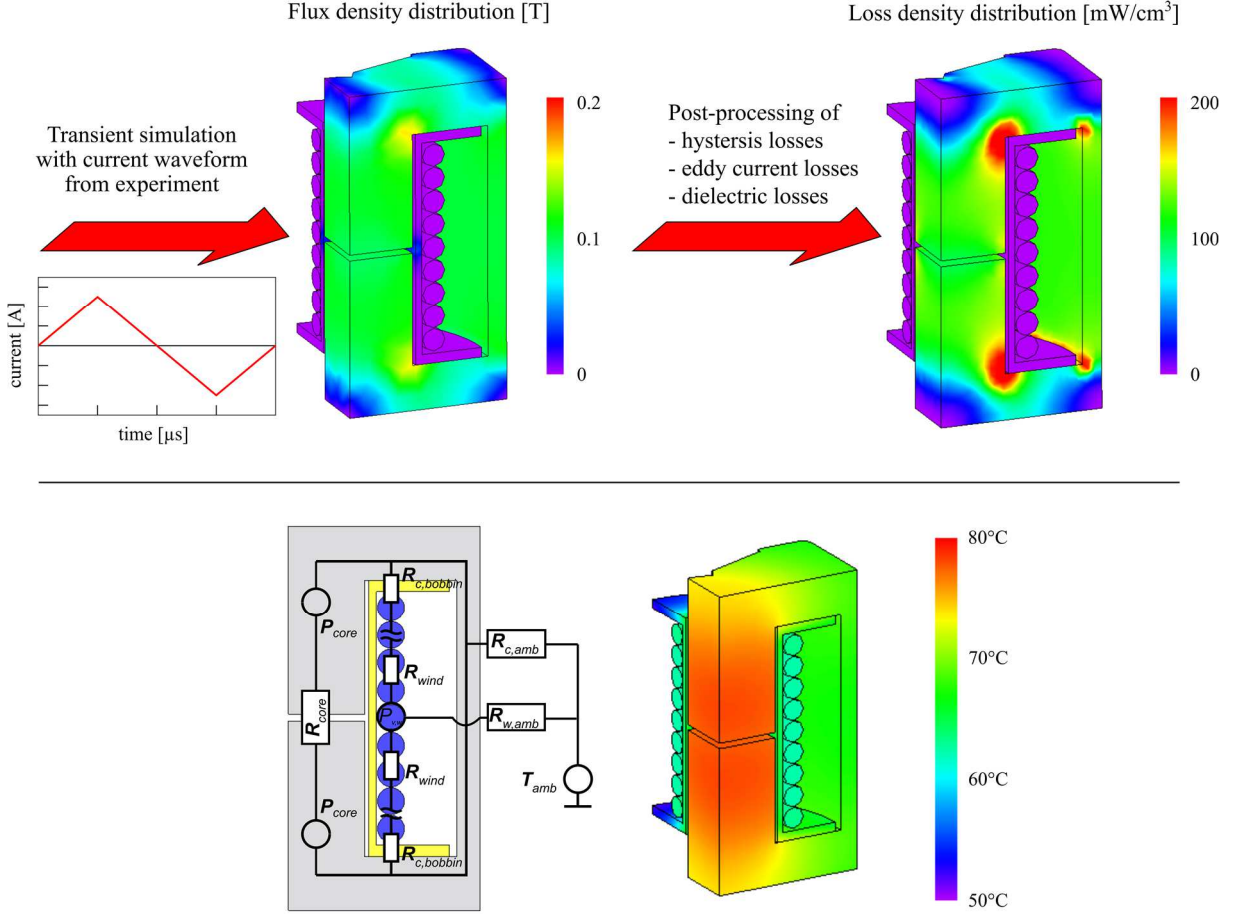


Fig. 6: 3D-FEM-Simulation results of a PQ50-core; top: Workflow of the simulation based on calculation of the core-losses; bottom: Simplified equivalent thermal circuit and temperature distribution of the component.

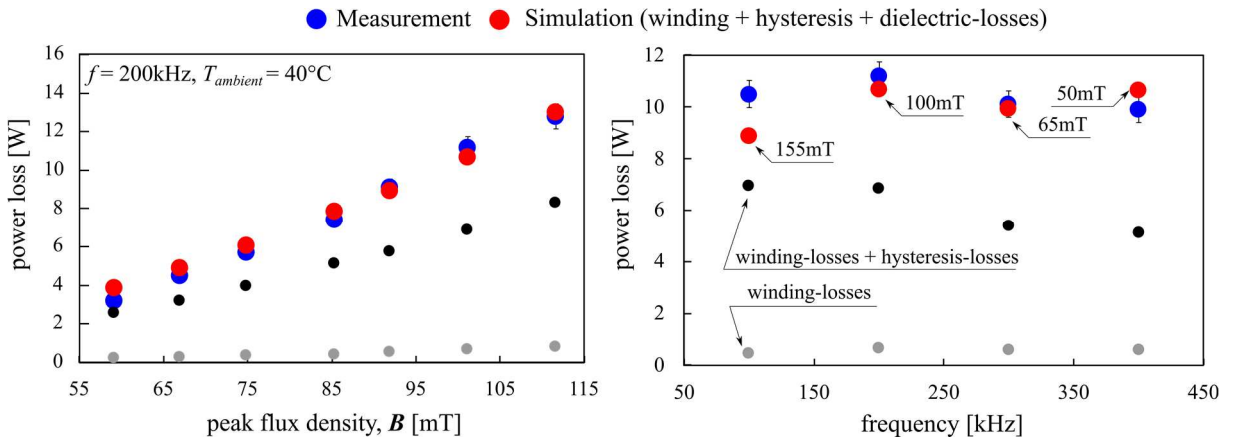


Fig. 7: Comparison of simulated (dark red) and measured (blue) losses for different flux-densities and frequencies. The error bars indicated a 5 % deviation of the measured values.

The accuracy can be increased when the dielectric volume losses introduced above are added to the core losses indicated by the dark red circles in Fig. 7. Therefore, the polarization loss ($\epsilon''_{\text{dipol}} = 35000$) is assumed to be independent of the frequency and temperature which can be seen from

Fig. 5. The resistivity/conductivity loss ($\rho = 1.66 \Omega\text{m}$) of the material is calculated for 100 °C with the constant taken from Table I. The precision of the simulation results is now discussed for the point of operation with a maximum flux-density of 100 mT and a frequency of 200 kHz. Here the difference between the measured and calculated losses is about 4.3 W when considering classical low volume losses only. The resulting additional losses due to conductivity and polarization losses are calculated to 2.3 W and 1.6 W, respectively by using the flux-density distribution of the FEM-simulation. The form-factor of the PQ-core is taken from the round-shaped magnetic cross-section valid in the center-leg. Thus, the total calculated losses in the component are approximately 10.8 W and, hence, about 0.5 W lower than the measured value of 11.3 W. This procedure is repeated for all operating points and the overall achievable accuracy in the investigated range is approximately 85 % to 90 %.

Finally, the uncertainties of the approach are discussed. The specific resistivity of the material is taken for a temperature of 25 °C. It is known that it decreases with the temperature and consequently. The temperature and frequency dependence of ε''_{dipol} needs to be investigated further and implemented in the simulation workflow. However, the results presented here show that the used numbers are reasonable in the investigated range. Consequently, the work presented here shows that the losses of cores with non-toroidal shapes can be predicted with significant accuracy. This gives rise to using FEM-simulations as a powerful tool in an industrial development process for magnetic components for automotive applications. In the future, accurate virtual prototypes can be generated and can substitute cost- and time-consuming hardware-loops.

Conclusion

To conclude, core-loss mechanisms for large-scale ferrite cores are investigated in this paper. It is demonstrated that for cores with cross-sections much higher than that used for datasheet measurements and at frequencies above hundred kHz additional loss mechanisms become significant. In order to accurately predict the losses of such cores, a model is presented which allows the calculation of the dielectric losses which vanish for small cores.

The model is analyzed in the framework of an extensive experimental study of test-structures of different geometries in wide range of frequency, temperature, and flux-density. By splitting the dielectric loss ε''_r in a part of conductivity loss $\sigma/(\omega\varepsilon_0)$ and in a part of polarization loss ε''_{dipol} the calculated data can be fitted to the measurement results to determine these parameters. Surprisingly, a good agreement between the measurement and the model can be achieved just with single numbers for each material.

In another measurement of test structures, the polarization loss is determined experimentally. The results give rise that the polarization losses can be calculated in a wide frequency and temperature range with a material specific but constant parameter. In addition, it is shown that the conductivity losses are temperature dependent and can be modeled using the Arrhenius-equation. Consequently, the findings presented in this paper give rise to calculate the additional dielectric volume losses over a wide frequency and temperature range with just two additional parameters.

The model is finally tested with the calculation of the core losses based on 3D-FEM-simulation results and compared to calorimetric measurements. The essential parameters for the FEM-simulation can be used from the experiments presented above. The simulations are in good agreement with the calorimetric measurements and show that core-losses can be predicted with an accuracy of several per cent by considering all loss-mechanisms.

References

- [1] C. Drexler, M. Wohlstreicher, P. Wrensch, H. Jungwirth and M. Schmidhuber. "Calculation and verification of high-frequency losses in power inductors for automotive application", PCIM Europe digital days, Nuremberg, Germany, 2021, Part of ISBN: 978-3-8007-5515-8.
- [2] M. Albach. "Induktivitäten in der Leistungselektronik", Springer Fachmedien Wiesbaden GmbH, Wiesbaden, Germany, 2017, DOI: 10.1007/978-3-658-15081-5.
- [3] P. Zacharias. "Magnetic Components", Springer Nature, Wiesbaden, Germany, 2022, ISBN: 978-3-658-37205-7.
- [4] E.C. Snelling. "Soft Ferrites: Properties and Applications", Iliffe Books Ltd, London, UK, 1969, ISBN: 978-0-592-02790-6
- [5] M. Kacki, M. S. Ryłko, J. G. Hayes and Ch. Sullivan. "A Study of Flux Distribution and Impedance in Solid and Laminar Ferrite Cores", IEEE Applied Power Electronics Conference and Exposition (APEC), Anaheim, CA, USA, 2019, DOI: 10.1109/APEC.2019.8722252.
- [6] T. Dimier and J. Biela. "Eddy Current Loss Model for Ferrite Ring Cores based on a Meta-Material Model for the Core Properties", IEEE Transactions on Magnetics, Vol. 58, No. 2, 2022, DOI: 10.1109/TMAG.2021.3084812.
- [7] J. Kita, K. Hashimoto, Y. Takahashi, K. Fujiwara, Y. Ishihara, A. Ahagon, T. Matsuo. "Magnetic Field Analysis of Ring Core Taking Account of Hysteretic Property Using Play Mode", IEEE Transactions on Magnetics, Vol. 48, No. 11, pp. 3375-3378, 2012, DOI: 10.1109/TMAG.2012.2204045.
- [8] D. C. Jiles and D. L. Atherton. "Theory of ferromagnetic hysteresis", Journal of Magnetism and Magnetic Materials, Vol. 61, No. 1-2, pp. 48-60, 1986, DOI: 10.1016/0304-8853(86)90066-1
- [9] A. Stadler. "Messtechnische Bestimmung und Simulation der Kernverluste in weichmagnetischen Materialien", Ph.D. thesis, Friedrich-Alexander-Universität Erlangen-Nürnberg, Erlangen, Germany, 2009.
- [10] J. R. Macdonald. "Impedance Spectroscopy - Emphasizing Solid Materials and Systems", John Wiley & Sons Inc, New York, NY, USA, 1987, ISBN: 978-0-471-83122-8
- [11] M. Kacki, M. S. Ryłko, J. G. Hayes and Ch. Sullivan. "A Practical Method to Define High Frequency Electrical Properties of MnZn Ferrites", IEEE Applied Power Electronics Conference and Exposition (APEC), New Orleans, LA, USA, 2020, DOI: 10.1109/APEC39645.2020.9124101
- [12] W. Kampczyk and E. Röß. "Ferritkerne : Grundlagen, Dimensionierung, Anwendungen in der Nachrichtentechnik", Siemens AG Berlin München, Berlin, Germany, 1978, ISBN: 978-3-800-91254-4
- [13] https://e-magnetica.pl/thermal_resistance_of_ferrite_cores, 31.05.2022, 10:16.